RAA 2017 Vol. **17** No. **8**, 78 (10pp) doi: 10.1088/1674–4527/17/8/78

http://www.raa-journal.org *http://iopscience.iop.org/raa*

Research in Astronomy and Astrophysics

The snowline in the protoplanetary disk and extrasolar planets

Chun-Jian Liu[1†], Zhen Yao[2] and Wen-Bo Ding[3]

[1] College of Mathematics and Physics, Bohai University, Jinzhou 121013, China; *chunjianjlu@163.com*
[2] College of Science, Liaoning University of Technology, Jinzhou 121001, China; *yaozhenjlu@163.com*
[3] College of Mathematics and Physics, Bohai University, Jinzhou 121013, China; *dingwenbo1980@163.com*

Received 2016 October 15; accepted 2017 March 31

Abstract We investigate the behavior of the snowline in a protoplanetary disk and the relationship between the radius of the snowline and properties of molecular cloud cores. In our disk model, we consider mass influx from the gravitational collapse of a molecular cloud core, irradiation from the central star, and thermal radiation from the ambient molecular cloud gas. As the protoplanetary disk evolves, the radius of the snowline increases first to a maximum value $R_{\max}$, and then decreases in the late stage of evolution of the protoplanetary disk. The value of $R_{\max}$ is dependent on the properties of molecular cloud cores (mass $M_{\rm core}$, angular velocity ω and temperature $T_{\rm core}$). Many previous works found that solid material tends to accumulate at the location of the snowline, which suggests that the snowline is the preferred location for giant planet formation. With these conclusions, we compare the values of $R_{\max}$ with semimajor axes of giant planets in extrasolar systems, and find that $R_{\max}$ may provide an upper limit for the locations of the formation of giant planets which are formed by the core accretion model.

Key words: snowline — planets and satellites: formation — protoplanetary disks

1 INTRODUCTION

The snowline plays a vital role during the evolution of a protoplanetary disk in various astrophysical processes, such as the distribution of water and formation of gas giant planets. The snowline is defined as the radius where the disk temperature is equal to the sublimation/condensation temperature of water-ice in the protoplanetary disk. Inside the snowline, water-ice will be evaporated into water vapor. Outside the snowline, water-ice, which is the most abundant species of solid, is present due to the condensation of water vapor. The surface density of solids, $\Sigma_{\rm s}$, is thus rapidly and significantly enhanced. In the core accretion model of giant planet formation (Lissauer 1993), a high value of $\Sigma_{\rm s}$ is needed to produce the solid cores of giant planets on a timescale consistent with the lifetime of the protoplanetary disk. Thus, the snowline is important to the formation of giant planets.

Stevenson & Lunine (1988) first proposed a mechanism which significantly enhances the surface density of solid material in the region of Jupiter using the effect of the snowline. Due to the diffusive redistribution of water vapor from the inner region of the solar nebula to the snowline and the condensation of water vapor outside the snowline, they found that the surface density of solids immediately outside of the snowline increases by a factor of $\sim$75 in roughly 10^5 yr. After reaching the snowline, the water vapor was assumed to condense into ice and be accreted by the pre-existing planetesimals located there. This enhancement of solid material is enough to produce the solid core of Jupiter on a short timescale and to trigger the rapid gas accretion phase of the core accretion model (Pollack et al. 1996) within the lifetime of the protoplanetary disk.

Stepinski & Valageas (1997) investigated the global evolution of solid material in a turbulent protoplanetary disk, and found that the radial distribution of solid material in the protoplanetary disk ends in the formation of the planetesimal swarm whose inner edge is nearly the snowline. This planetesimal swarm provides a large amount of material which produces the solid cores of giant planets on a short timescale. Haghighipour & Boss (2003)

† Corresponding author.

studied the inward and outward migration of small solids in the vicinity of the local pressure enhancement in a gaseous nebula. These solids range from micron-sized dust grains to meter-sized objects. They found that, with the combined effects of gas drag and pressure gradients, solids migrate to the locations of the local pressure enhancement and accumulate there. This causes the surface density of solids at the maximum-pressure location to increase significantly. Cuzzi & Zahnle (2004) found that icy material from the outer region of the disk evaporates when migrating inward across the snowline. Since water vapor from the sublimation of icy material cannot be removed as fast as it is being supplied in solid form, the concentration of vapor increases significantly and creates a local enhancement of gas near the snowline. Thus solid particles tend to accumulate near the snowline and produce planetesimals.

Kretke & Lin (2007) proposed a mechanism for the accumulation of solid particles and the formation of planetesimals near the snowline in a magneto-rotational instability (MRI) turbulence-driven disk. Because MRI can only occur in the surface layer of the disk (Gammie 1996), there is a sharp change in the grain-to-gas density ratio across the snowline. This change creates a local maximum in the radial distribution of the gas surface density and pressure near the snowline, which causes the retention of solid particles and the formation of planetesimals near the snowline. Ciesla & Cuzzi (2006) also found a planetesimal swarm outside the snowline. Zhang et al. (2015) found that the observed emission dip in long baseline 2.9, 1.3 and 0.87 mm continuum images of the young star HL Tau is caused by the rapid growth of pebbles near the snowline, due to the accumulation of solid particles there. Thus the snowline is a preferred location of planet formation and can be used to estimate the semimajor axes of giant planets.

In this paper, we explore evolution of the snowline in a protoplanetary disk by considering the mass influx from a molecular cloud core. The radius of the snowline $R_{\rm snow}$ increases first to a maximum value $R_{\rm max}$, and then decreases with time. This behavior is due to mass influx from the molecular cloud core. The maximum value of the radius of the snowline $R_{\rm max}$ is dependent on properties of the molecular cloud core (mass $M_{\rm core}$, angular velocity ω and temperature $T_{\rm core}$). We propose that $R_{\rm max}$ is the preferred location of planet formation, and compare $R_{\rm max}$ with the semimajor axes of extrasolar planets. We find that $R_{\rm max}$ is compatible with the semimajor axes of extrasolar planets.

This paper is organized as follows. In Section 2, we describe our disk model. In Section 3, we calculate the evolution of the snowline $R_{\rm snow}$ through the lifetime of a protoplanetary disk. The radius of the snowline $R_{\rm snow}$ increases first to a maximum value $R_{\rm max}$, and then decreases with time. We show the dependence of $R_{\rm max}$ on the properties of molecular cloud cores and propose that $R_{\rm max}$ is the preferred location of giant planet formation. In Section 4, we compare the values of $R_{\rm max}$ with observed semimajor axes of extrasolar planets. In Section 5, we present our discussions and conclusions.

2 THE PROTOPLANETARY DISK MODEL

2.1 Properties of a Molecular Cloud Core

Standard star formation theory shows that a protoplanetary disk is formed from the collapse of a molecular cloud core (McKee & Ostriker 2007). Bacmann et al. (2000) and Shu (1977) found that an isothermal sphere is a good fit for the structure of a molecular cloud core with a density distribution $\rho(r) = (a^2/2\pi G)r^{-2}$ (Shu 1977), where r is the radial distance from the center, a is the isothermal sound speed in the cloud core and G is the gravitational constant. Molecular cloud cores are observed to have a slight rotation (Goodman et al. 1993). A molecular cloud core can be characterized by its angular velocity ω, mass $M_{\rm core}$ and temperature $T_{\rm core}$. With the above density distribution, the angular momentum of a molecular cloud core is

$$J = \frac{G^2\mu_1^2}{18R_{\rm g}^2}\frac{M_{\rm core}^2\omega}{T_{\rm core}^2}, \quad (1)$$

where μ_1 is the mean molecular weight which we set to be 2.33, and $R_{\rm g}$ is the gas constant. The self-similar solution of the gravitational collapse of a molecular cloud core results in a mass infall rate onto the protoplanetary disk+protostar system as $\dot{M}_{\rm core} = 0.975a^3/G = (0.975/G)(R_{\rm g}/\mu_1)^{3/2}T_{\rm core}^{3/2}$ (Shu 1977). For a given $T_{\rm core}$, the collapse timescale of a molecular cloud core is

$$\begin{aligned} t_{\rm infall} &= \frac{M_{\rm core}}{\dot{M}_{\rm core}} \\ &= \left(\frac{0.975}{G}\right)^{-1}\left(\frac{R_{\rm g}}{\mu_1}\right)^{-3/2} M_{\rm core}T_{\rm core}^{-3/2}. \end{aligned} \quad (2)$$

When time t is larger than $t_{\rm infall}$, gravitational collapse of the molecular cloud core stops. The molecular cloud core provides the initial condition and mass influx for the evolution of the protoplanetary disk+protostar system. The core properties ($M_{\rm core}$, ω and $T_{\rm core}$) determine the evolution of the protoplanetary disk. Goodman et al. (1993) observed that ω is in the range of $0.1 - 13 \times 10^{-14}\,{\rm s}^{-1}$ with a median value of $2.8 \times 10^{-14}\,{\rm s}^{-1}$. Jijina et al.

(1999) observed that the temperature $T_{\rm core}$ is in the range 7–40 K with a median value of 15 K. Motte et al. (1998) observed that $M_{\rm core}$ is in the range of ∼0.1–3 $M_\odot$ with a median value of 1 $M_\odot$.

2.2 The Disk Model

Here we develop a more realistic and reasonable disk model based on the disk model of Jin & Sui (2010), but with some improvements in optimization. We mainly make the following improvements: first, we adopt the thermal ionization results of Umebayashi (1983) to calculate the viscosity in the inner region of the disk, rather than the criterion of 800 K; second, we adopt the results of Kratter et al. (2008) to calculate the viscosity caused by gravitational instability, rather than the global model of Laughlin & Bodenheimer (1994) and Laughlin & Rozyczka (1996); third, we adopt irradiation from the central star from Zhu et al. (2012) rather than from Hueso & Guillot (2005); fourth, we adopt thermal radiation from the molecular cloud gas from Ciesla & Cuzzi (2006), not from Jin & Sui (2010); finally, we use the radius of the central star $R_* = 2.6\,R_\odot$ and the effective temperature on the surface of the central star $T_* = 4280$ K from Fukue (2013), not the values $R_* = 0.012$ AU and $T_* = 4500$ K from Hueso & Guillot (2005). We review the disk model of Jin & Sui (2010) below. Nakamoto & Nakagawa (1994) derived the mass flux onto the disk of a collapsing molecular cloud core from Cassen & Moosman (1981),

$$S(R,t) = \begin{cases} \frac{\dot{M}_{\rm core}}{4\pi R R_{\rm d}(t)} \left[1 - \frac{R}{R_{\rm d}(t)}\right]^{-1/2} & \text{if } R < R_{\rm d}(t); \\ 0 & \text{otherwise,} \end{cases} \tag{3}$$

where $R_{\rm d}(t)$ is the centrifugal radius, R is the cylindrical radius and t is the time. $R_{\rm d}(t)$ is given by

$$\begin{aligned} R_{\rm d}(t) &= \frac{1}{16} a\omega^2 t^3 \\ &= 53.6 \left(\frac{\omega}{10^{-14}{\rm s}^{-1}}\right)^2 \left(\frac{T_{\rm core}}{10\,{\rm K}}\right)^{1/2} \\ &\quad \times \left(\frac{t}{6\times10^5\,{\rm yr}}\right)^3 \ {\rm AU}. \end{aligned} \tag{4}$$

When the mass of the cloud core is depleted, the collapse stops.

The basic equation which describes the evolution of the surface density of a protoplanetary disk is derived from Jin & Sui (2010)

$$\begin{aligned} \frac{\partial \Sigma}{\partial t} &= \frac{3}{R}\frac{\partial}{\partial R}\left[R^{1/2}\frac{\partial}{\partial R}\left(\Sigma\nu R^{1/2}\right)\right] \\ &\quad + S(R,t) + S(R,t)\Bigg\{2 - 3\left[\frac{R}{R_{\rm d}(t)}\right]^{1/2} \\ &\quad + \frac{R/R_{\rm d}(t)}{1+\left[R/R_{\rm d}(t)\right]^2}\Bigg\}, \end{aligned} \tag{5}$$

where Σ is the gas surface density of the disk and ν is the kinematic viscosity. The second term on the right hand side of Equation (5) is the mass influx caused by the collapse of the cloud core. The last term appears as a result of the difference in specific angular momentum between the infalling material and the material already residing in the disk. We use the alpha prescription $\nu = \alpha c_{\rm s} H$ of Shakura & Sunyaev (1973) to calculate the viscosity ν, where $c_{\rm s}$ is the local sound speed, H is the half thickness of the disk and α is a dimensionless parameter. In this paper, we adopt the following formula for α,

$$\alpha = \begin{cases} \alpha_{\rm GI} + \alpha_{\rm MRI} & \text{if } \alpha_{\rm GI} + \alpha_{\rm MRI} > \alpha_{\rm min}; \\ \alpha_{\rm min} & \text{otherwise,} \end{cases} \tag{6}$$

where $\alpha_{\rm GI}$ is the viscosity induced by gravitational instability, $\alpha_{\rm MRI}$ is the viscosity induced by MRI and $\alpha_{\rm min}$ is the minimum value of α when both MRI and gravitational instability are absent.

When gravitational instability occurs in the protoplanetary disk, viscosity is enhanced by a large factor. Gravitational instability of the protoplanetary disk is judged using the Toomre-Q parameter (Toomre 1964),

$$Q = \frac{c_{\rm s}\Omega}{\pi G\Sigma}, \tag{7}$$

where Ω is the Keplerian angular velocity in the disk. Gravitational instability occurs when Q is smaller than $Q_{\rm crit}$. Otherwise, gravitational instability does not occur. In this paper, we set $Q_{\rm crit}$ to be 2.0 according to Kratter et al. (2008). The following formula of α_{GI} is adopted (Kratter et al. 2008),

$$\alpha_{\rm GI} = \left(\alpha_{\rm short}^2 + \alpha_{\rm long}^2\right)^{1/2}, \tag{8}$$

where

$$\alpha_{\rm short} = \max\left[0.14\left(\frac{1.3^2}{Q^2} - 1\right)(1-\mu)^{1.15}, 0\right], \tag{9}$$

and

$$\alpha_{\rm long} = \max\left[\frac{1.4\times10^{-3}\,(2-Q)}{\mu^{5/4}Q^{1/2}}, 0\right], \tag{10}$$

where $\mu = M_{\rm disk}/(M_{\rm disk}+M_*)$ is the disk-to-total mass ratio, $M_{\rm disk}$ is the mass of the disk, and M_* is the mass of

the central star. We take $Q = \max[Q, 1]$ in Equation (9) and Equation (10) according to Kratter et al. (2008).

When $Q > 2.0$, gravitational instability does not occur, and the dominant viscosity is due to MRI (Balbus & Hawley 1991). We adopt the results of Fleming & Stone (2003) and Umebayashi (1983) to calculate $\alpha_{\rm MRI}$. The disk can be divided into three regions based on different mechanisms of viscosity (Jin & Sui 2010). In the inner region, the temperature is high enough to cause thermal ionization and MRI can occur. We adopt results of Umebayashi (1983) to calculate the viscosity caused by thermal ionization, rather than the 800 K criterion found in Jin & Sui (2010). In the outer region, the disk material is rarefied enough to be penetrated by cosmic rays. These cosmic rays can cause ionization. MRI can also occur in the outer region and cause high viscosity (Fleming & Stone 2003). In the intermediate region, the temperature is not high enough to cause thermal ionization and the disk material is not rarefied enough to be entirely penetrated by cosmic rays. Thus the disk displays "layered accretion" (Gammie 1996). MRI can only occur in the surface layer of the disk, and the remaining part is inactive with respect to MRI (called the "dead zone"). In this region, we adopt a viscosity of hydrodynamic processes, $\alpha_{\rm min}$, to drive the disk evolution. In this work, we set $\alpha_{\rm min}$ to be 10^{-4}, which is the median order of magnitude in Chambers (2006), Dubrulle (1993), Klahr & Bodenheimer (2003), Richard (2003) and Dubrulle et al. (2005).

We use the balance of energy to calculate temperature in the disk. The heating sources include: viscous dissipation, irradiation from the protostar (Zhu et al. 2012), shock heating of the infalling material from mass influx onto the disk (Jin & Sui 2010) and thermal radiation from the ambient molecular cloud gas (Ciesla & Cuzzi 2006). Surface temperature is obtained using the balance of surface radiation flux and heating sources as in Nakamoto & Nakagawa (1994),

$$\sigma T_{\rm s}^4 = \frac{1}{2}\left(1+\frac{1}{2\tau_{\rm p}}\right)\left(\dot{E}_{\rm v}+\dot{E}_{\rm s}\right)+\sigma T_{\rm ir}^4+\sigma T_{\rm core}^4, \tag{11}$$

where σ is the Stefan-Boltzmann constant, $T_{\rm s}$ is the surface temperature of the disk, $\dot{E}_{\rm v} = \frac{9}{4}\Sigma\bar{\nu}\Omega^2$ is the viscous dissipation rate,

$$\dot{E}_{\rm s} = S(R,t)\Big[e_{\rm core}(R,t) - e_{\rm dist}(R,t)\Big]$$

is the energy generation rate by shock heating, $\sigma T_{\rm ir}^4$ is irradiation from the protostar (Zhu et al. 2012) and $\sigma T_{\rm core}^4$ is thermal radiation from the ambient molecular cloud gas (Ciesla & Cuzzi 2006). $\tau_{\rm p} = k_{\rm p}\Sigma/2$ is the Planck mean optical depth and $k_{\rm p}$ is the Planck mean opacity. Irradiation from the protostar is adopted from Zhu et al. (2012),

$$T_{\rm ir}^4 = \frac{f(R)L_*}{4\pi R^2\sigma}, \tag{12}$$

where $f(R) = 0.1$ accounts for the normal component of irradiation from the central star to the disk and $L_* = 4\pi R_*^2\sigma T_*^4$ is the luminosity on the surface of the central star. $R_* = 2.6\,R_\odot$ (Fukue 2013) is radius of the central star, and $T_* = 4280\,{\rm K}$ (Fukue 2013) is effective temperature on the surface of the central star. With the radiative diffusion approximation the midplane temperature $T_{\rm m}$ is (Nakamoto & Nakagawa 1994)

$$\sigma T_{\rm m}^4 = \frac{1}{2}\left[\left(\frac{3}{8}\tau_{\rm R}+\frac{1}{2\tau_{\rm p}}\right)\dot{E}_{\rm v}+\left(1+\frac{1}{2\tau_{\rm p}}\right)\dot{E}_{\rm s}\right] +\sigma T_{\rm ir}^4+\sigma T_{\rm core}^4, \tag{13}$$

where $\tau_R = k_R\Sigma/2$ is the Rosseland mean optical depth, and $k_{\rm R}$ is the Rosseland mean opacity. The Rosseland mean opacity is adopted from Bell & Lin (1994) and Bell et al. (1997).

3 BEHAVIOR OF THE SNOWLINE IN THE PROTOPLANETARY DISK

We calculate the temperature of the disk using Equations (11) and (13). We adopt the conventional criterion to determine the location of the snowline, that is, the midplane temperature $T_{\rm m}$ is equal to the sublimation/condensation temperature of water-ice in the protoplanetary disk, 170 K (Hayashi 1981). However, this conventional criterion to determine the location of the snowline is not strictly correct. In equilibrium at which the water condensation rate onto an ice grain is equal to the sublimation rate from the grain, the condensation temperature of water vapor is equal to the temperature of the gas and the 170 K criterion is suitable in this case.

Podolak & Mekler (1997) computed the temperature of dirty ice grains by considering the heating processes (solar radiation and the impact of water molecules) and the cooling processes (reradiation and vaporization) of dirty ice grains. They found the possibility of having grains with a layer of amorphous ice surrounded by a layer of crystalline ice. Podolak & Zucker (2004) computed the temperature of pure ice grains and dirty ice grains in a protoplanetary disk based on the model of Podolak & Mekler (1997). The heating processes arise from solar radiation and the impact of water molecules. The cooling processes come from the reradiation, the sublimation of water molecules from the grain surface and the contact with gas in the disk. They found that

the condensation temperature of water vapor is not always 170 K in some cases. Thus the 170 K criterion of the snowline is not always strictly correct. However, a detailed calculation of the temperature of ice grains is beyond the scope of this paper, and the purpose of this paper is to give an illustrative description of the general varying trend of the snowline and dependence of the snowline on properties of the molecular cloud core. Thus the accuracy of the 170 K criterion of the snowline is enough for our purposes, and we tend to adopt the 170 K criterion to determine the location of the snowline.

Figure 1 shows the evolution of radius of the snowline $R_{\rm snow}$ with different ω values, $M_{\rm core} = 1\ M_{\odot}$ and $T_{\rm core} = 15$ K. The time t is expanded to the lifetime of the protoplanetary disk, 6×10^6 yr (Haisch et al. 2001). We find that the radius of the snowline $R_{\rm snow}$ increases first in the early stage of the disk's evolution, reaches a maximum value at time $\sim t = 3.46 \times 10^5$ yr, and then decreases with time in the later stage of the disk's evolution. The physical reason is as follows. In the early stage of disk evolution, the mass flux $S(R,t)$ continuously supplies infalling material to the disk and heats the disk material by way of shock heating the disk material. The increased amount of material causes more viscous heating. Thus the radius of the snowline $R_{\rm snow}$ increases at the early stage of disk evolution due to mass influx $S(R,t)$. When the mass influx stops at $t_{\rm infall} = 3.46 \times 10^5$ yr, $R_{\rm snow}$ reaches the maximum value $R_{\rm max}$ (Fig. 1). After time instant $t_{\rm infall}$, the disk evolution enters into an isolated stage without mass influx. The disk material is continuously accreted onto the central star and the viscous heating consequently decreases. The radius of the snowline $R_{\rm snow}$ begins to decrease at the late stage of disk evolution due to cooling and accretion of the disk (Fig. 1).

From Figure 1, the maximum radius of the snowline $R_{\rm max}$ is an important characteristic of the evolutionary behavior of the snowline as well as of the overall heating of the protoplanetary disk. Next, we investigate the behaviors of $R_{\rm max}$ and focus on the dependence of $R_{\rm max}$ on parameters of molecular cloud cores (ω, $T_{\rm core}$ and $M_{\rm core}$).

In Figure 2, we show the dependence of maximum radius of the snowline $R_{\rm max}$ on angular velocity ω of the molecular cloud core. In this figure, the maximum radius of the snowline $R_{\rm max}$ increases first with ω, reaches its maximum at $\omega = 2.0 \times 10^{-14}\ {\rm s}^{-1}$ and then decreases with ω when $\omega > 2.0 \times 10^{-14}\ {\rm s}^{-1}$. The physical reason is as follows. When the value of ω is zero, angular momentum of the total protoplanetary disk+protostar system is zero, and the molecular cloud core collapses directly onto the central star without the protoplanetary disk existing. As ω increases, the angular momentum of the total protoplanetary disk+protostar system increases (Eq. (1)). The increased total angular momentum leads to an increase in kinetic energy of the disk material and more material in the disk. The increased material (high Σ) in the disk generates more viscous heating to heat the disk material, and simultaneously, increased kinetic energy also heats the disk material. Since $R_{\rm max}$ characterizes the overall heating of the disk, it increases with ω. However, after ω increases to $2.0 \times 10^{-14}\ {\rm s}^{-1}$, the high total angular momentum extends the region of the protoplanetary disk too much. As the disk material is extended to very large radii, it becomes rarefied and viscous heating decreases. Additionally, when the total angular momentum increases to a high enough value, gravitational instability (Kratter et al. 2008) and fragmentation (Gammie 2001) will occur in the protoplanetary disk. These effects will also cool the disk on a short timescale. Thus, $R_{\rm max}$ decreases when ω is too high.

In Figure 3, we show the dependence of maximum radius of the snowline $R_{\rm max}$ on temperature of the molecular cloud core $T_{\rm core}$. The relation of the maximum radius of the snowline $R_{\rm max}$ on the temperature $T_{\rm core}$ is similar to that on angular velocity ω, first increasing to a maximum value and then decreasing. But the physical reason is different. The thermal irradiation from ambient molecular cloud core gas $\sigma T_{\rm core}^4$ is included as a heating source (Eq. (13)). As the temperature of the molecular cloud core $T_{\rm core}$ increases, thermal irradiation from the ambient molecular cloud core gas also increases. This increases the heating of the disk material, and the maximum radius of the snowline $R_{\rm max}$ increases. However, as the temperature $T_{\rm core}$ increases continuously, the total angular momentum of the protostar+disk system decreases (Eq. (1)). The decreased angular momentum cannot spread a large amount of infalling material in the protoplanetary disk and the amount of material in the disk decreases. The reduced amount of material in the protoplanetary disk consequently decreases the viscous heating source. Thus, with competition between thermal irradiation from the ambient molecular cloud core gas and total angular momentum of the protostar+disk system, the maximum radius of the snowline $R_{\rm max}$ first increases and then decreases with the temperature of the molecular cloud core $T_{\rm core}$.

In Figure 4, we show the dependence of maximum radius of the snowline $R_{\rm max}$ on the mass of molecular cloud core $M_{\rm core}$. Unlike its relationship with angular velocity ω and temperature $T_{\rm core}$, $R_{\rm max}$ increases monotonically with the mass $M_{\rm core}$ and has an asymptotic value of $\sim$13.17 AU. The physical reason is as fol-

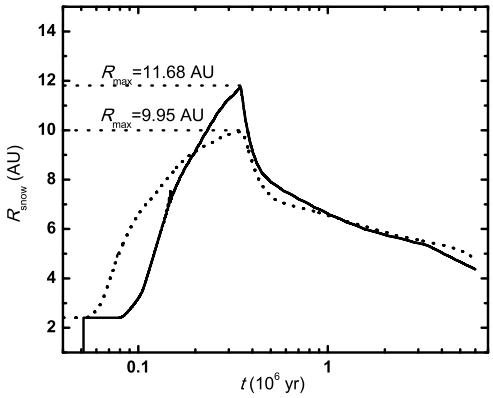

Fig. 1 Radius of the snowline $R_{\rm snow}$ versus the evolution time t with different ω values, $M_{\rm core} = 1\,M_{\odot}$ and $T_{\rm core} = 15$ K. The solid line represents the radius of the snowline with $\omega = 2.8 \times 10^{-14}$ s^{-1} and the dotted line represents the radius of the snowline with $\omega = 6.0 \times 10^{-14}$ s^{-1}.

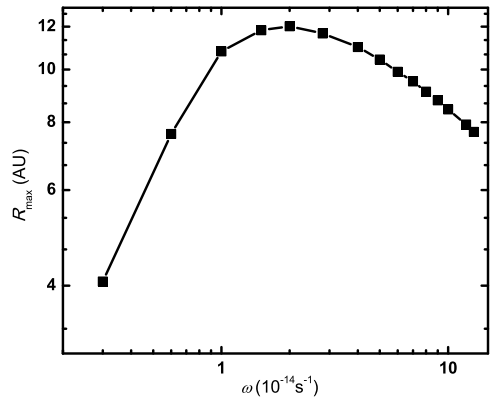

Fig. 2 The maximum radius of the snowline $R_{\rm max}$ versus ω with typical values $M_{\rm core} = 1\,M_{\odot}$ and $T_{\rm core} = 15$ K. The value of ω is in the observational range of $0.1 - 13 \times 10^{-14}$ s^{-1} (Goodman et al. 1993).

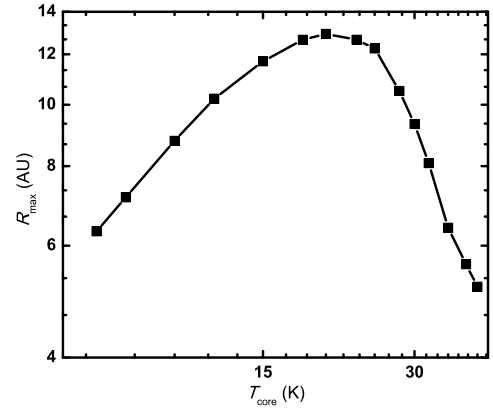

Fig. 3 The maximum radius of the snowline $R_{\rm max}$ versus $T_{\rm core}$ with typical values $M_{\rm core} = 1\,M_{\odot}$ and $\omega = 2.8 \times 10^{-14}$ s^{-1}. $T_{\rm core}$ is in the observational range of 7–14 K (Jijina et al. 1999).

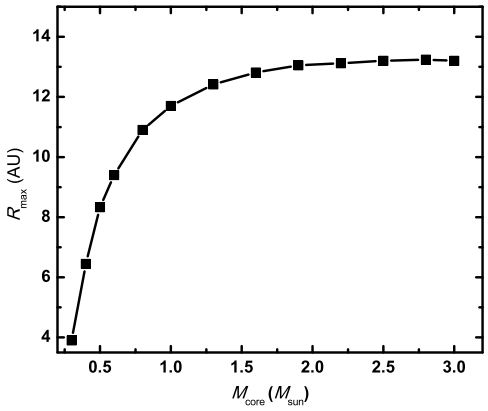

Fig. 4 The maximum radius of the snowline $R_{\max}$ versus $M_{\rm core}$ with typical values $T_{\rm core} = 15$ K and $\omega = 2.8 \times 10^{-14}\,{\rm s}^{-1}$. $M_{\rm core}$ is in the observational range of $\sim$0.1–3 $M_\odot$ (Motte et al. 1998).

lows. As the mass $M_{\rm core}$ increases, the amount of material and angular momentum of the disk+protostar system increase simultaneously. The surface density of the disk Σ increases continuously. This leads to a high viscous heating of the disk material and therefore the maximum radius of snowline $R_{\max}$ increases continuously. Although the high angular momentum spreads disk material to large radii, the increased mass $M_{\rm core}$ resupplies material in the extended disk region, thus the disk material does not become rarefied (low Σ), which causes viscous heating to increase continuously. Therefore, the maximum radius of the snowline $R_{\max}$ increases continuously with mass $M_{\rm core}$ without decreasing.

We have presented the dependence of maximum radius of the snowline $R_{\max}$ on parameters of the parent molecular cloud core (mass $M_{\rm core}$, angular velocity ω and temperature $T_{\rm core}$). The dependence of $R_{\max}$ on angular velocity ω and temperature $T_{\rm core}$ is similar, first increasing to a maximum value and then decreasing. However, $R_{\max}$ is a monotonically increasing function of mass $M_{\rm core}$ and has an asymptotic value of $\sim$13.17 AU. We have explained the physical reasons above.

4 IMPLICATIONS FOR THE FORMATION OF GIANT PLANETS

Maximum radius of the snowline $R_{\max}$ also has special significance for giant planet formation. From Stevenson & Lunine (1988), due to the diffusive redistribution of water vapor from the inner region of the solar nebula to the snowline and condensation of water vapor outside the snowline, the surface density of solids immediately outside of the snowline increases by a factor of $\sim$75 in roughly 10^5 yr. Stepinski & Valageas (1997) found that the radial distribution of solid material in the protoplanetary disk ends in the formation of a planetesimal swarm whose inner edge is nearly the snowline. This planetesimal swarm provides a large amount of the material which produces the solid cores of giant planets on a short timescale. Haghighipour & Boss (2003) found that, with the combined effects of gas drag and pressure gradients, solids migrate to the locations of local pressure enhancement and accumulate there. The location of the snowline satisfies the condition of local pressure enhancement. Cuzzi & Zahnle (2004) found that the concentration of vapor increases significantly and creates a local enhancement of gas near the snowline. Thus solid particles tend to accumulate near the snowline and produce planetesimals. Kretke & Lin (2007) found that, due to a sharp change in the grain-to-gas density ratio across the snowline, the radial distribution of gas surface density has a local maximum near the snowline, which causes the retention of solid particles and the formation of planetesimals near the snowline. Thus giant planets are most likely to be formed near the snowline. Note that the location of the snowline is proposed to be the preferred location of giant planet formation, but that is not to say the location of the snowline is the only location of giant planet formation. Giant planets can also be formed at other locations. The only difference is that the possibility of formation of giant planets near the snowline is maximum compared with other locations.

However, the radius of the snowline is fixed in the above works. In our disk model, the radius of the snowline $R_{\rm snow}$ first increases to a maximum $R_{\max}$ and then decreases with time. This is mainly due to mass influx from the molecular cloud core. According to Zhang & Jin (2015), $R_{\max}$ is a preferred location for the forma-

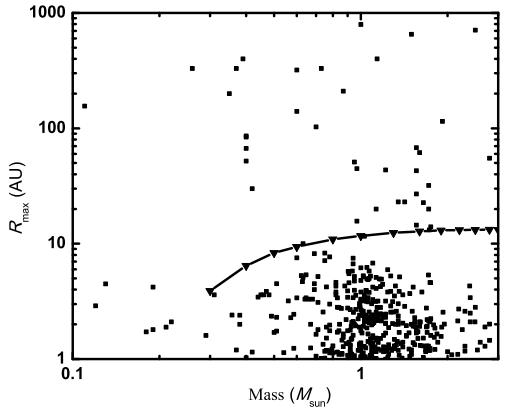

Fig. 5 Comparison between maximum radius of the snowline $R_{\rm max}$ and observed semimajor axes of extrasolar planets. The typical values of parameters are: $T_{\rm core} = 15$ K and $\omega = 2.8 \times 10^{-14}\,{\rm s}^{-1}$. The line with triangular symbols represents the maximum radii of the snowline $R_{\rm max}$, and squares represent the current extrasolar planetary catalog (*http://exoplanet.eu/*). The horizontal axis represents the mass of an exoplanet's host star, and the value corresponding to the $R_{\rm max}$ curve is $M_{\rm core}$. Note that the observed data on extrasolar planets include all known exoplanets with their associated masses. We only tend to exclude Hot Jupiters (semimajor axes < 1 AU), because we think they are formed in an unusual way. The selection criterion for extrasolar planets in Fig. 5 in our model is the semimajor axis, not the mass.

tion of giant planets due to the diffusion of water vapor. In the process of outward expansion of the snowline, water vapor also moves outward with the snowline due to the effects of diffusion. The water-ice which previously resided at a location outside the snowline will quickly sublimate after the snowline passes by this location. The sublimated ices will also be transported to the outward moving snowline due to the effects of diffusion. After the snowline reaches $R_{\rm max}$, the snowline moves inward and water-ice outside $R_{\rm max}$ will not sublimate. Thus, water vapor will tend to be transported to the maximum radius of the snowline $R_{\rm max}$ and accumulate there. This will produce a planetesimal swarm at the location of $R_{\rm max}$ on a short timescale (Stevenson & Lunine 1988; Ciesla & Cuzzi 2006). This planetesimal swarm will stop the inward migration of icy material beyond $R_{\rm max}$ and absorb this icy material to form a larger planetesimal swarm. Thus the location of $R_{\rm max}$ in our model is analogous to the conventional snowline in previous studies (Stevenson & Lunine 1988, Stepinski & Valageas 1997 and Kretke & Lin 2007). The maximum radius of the snowline $R_{\rm max}$ in our model could therefore be a preferred location for the formation of a giant planet in the core accretion model (Pollack et al. 1996). Note that, this is not to say giant planets cannot be formed at other locations. In fact, giant planets can also be formed at other locations. The only difference is that the possibility of the formation of giant planets near the snowline may be larger than at other locations. Giant planets can be formed at the location of $R_{\rm max}$ first, and then migrate inward to small semimajor axes. Moreover, we just adopt the maximum radius of the snowline $R_{\rm max}$ as a characteristic location of giant planet formation to give a visual picture of the correlation between the properties of molecular cloud cores and the observed semimajor axes of extrasolar planets. To exactly determine the location of the formation of giant planets needs more work.

In Figure 5, we compare the values of $R_{\rm max}$ with the observed semimajor axes of extrasolar planets. The observed data on extrasolar planets are adopted from the current extrasolar planetary catalog on 2016 June 1 (*http://exoplanet.eu/*). We tend to exclude extrasolar planets with semimajor axes smaller than 1 AU (Hot Jupiters), because these Hot Jupiters are conventionally thought to be formed by the core accretion model (Pollack et al. 1996) at large radii first, and then migrate inward to their present locations (Lin & Papaloizou 1986; Ida & Lin 2004). The core accretion+migration model can explain the presence of Hot Jupiters and the presence of a desert seen in observations. Note that the observed data on extrasolar planets include all the exoplanets with all the mass. We only tend to exclude Hot Jupiters (semimajor axes < 1 AU), because we think they are formed in an unusual way. The selection criterion for extrasolar planets in Figure 5 in our model is the semimajor axis, not the mass. On the other hand, Batygin et al. (2016) proposed a new mechanism in which Hot Jupiters can form in the inner region of the protoplanetary disk in situ

from existing Super-Earth type planets, which have 10–20 Earth masses of refractory material. In their model, Hot Jupiters can be formed on the close-in orbits from the protostar in situ, rather than experience long-range inward migration. However, the model of Batygin et al. (2016) is newly proposed and is not justified by much observational evidence. Thus we tend to adopt the conventional scenario for the formation of Hot Jupiters (Lin & Papaloizou 1986). We focus on the planet formation region of giant planets by the core accretion model from 1–10 AU. We can find that the values of $R_{\max}$ can provide an upper limit for the semimajor axes of extrasolar planets in the region 1–10 AU in general. Note that the location of $R_{\max}$ is just a preferred location for the formation of giant planets. Giant planets can also be formed at other locations. The only difference is that the possibility of the formation of giant planets near the snowline may be larger than at other locations. Giant planets can be formed at the location of $R_{\max}$ first, and then migrate inward to small semimajor axes. Thus $R_{\max}$ may provide an upper limit for the locations of the formation of giant planets which are formed by the core accretion model. In Figure 5, extrasolar planets above the $R_{\max}$ curve are indeed rare. This may provide some support for our model.

Additionally, the observed distribution should also be influenced by the limit of observations. Planets farther from the host star are more difficult to observe. The limit of observations may also have a role in the rarity of extrasolar planets beyond $\sim$10 AU. In the future, we would like to obtain more observational data on the semimajor axis distribution, and then the "boundary" seen in the semimajor axis distribution would disappear. Thus we think that the rarity of extrasolar planets beyond $\sim$10 AU may be caused by both the effect of $R_{\max}$ and the selection effect of the observation technique (namely, the limit of observations).

5 CONCLUSIONS AND DISCUSSION

In this paper, we investigate the behaviors of the snowline by considering mass influx from the molecular cloud core. We use a developed disk model based on the disk model of Jin & Sui (2010), but with some improvements in optimization. The snowline in our disk model first moves outward to a maximum radius $R_{\max}$, and then decreases with time. This behavior of the snowline is due to mass influx from gravitational collapse of the molecular cloud core. $R_{\max}$ characterizes the overall heating of the protoplanetary disk, and has special significance for giant planet formation. Solid particles tend to accumulate and form a planetesimal swarm near the snowline due to the local pressure maximum at the snowline (Stevenson & Lunine 1988, Stepinski & Valageas 1997). In our disk model, $R_{\max}$ is analogous to the conventional snowline in previous works. As stated above, $R_{\max}$ is a preferred location of giant planet formation. Note that, this is not to say giant planets cannot be formed at other locations. Giant planets can also be formed at other locations. The only difference is that the possibility of formation of giant planets near the snowline may be larger than at other locations. Giant planets can be formed at the location of $R_{\max}$ first, and then migrate inward to small semimajor axes. We come to the following conclusions:

(1) The radius of the snowline first moves outward to a maximum value $R_{\max}$ and then decreases with time. This is due to mass influx from the gravitational collapse of the molecular cloud core.
(2) The value of $R_{\max}$ first increases to a maximum value and then decreases with angular velocity of molecular cloud core ω. This is due to the extension of the disk region when ω becomes large.
(3) The value of $R_{\max}$ first increases to a maximum value and then decreases with temperature of the molecular cloud core $T_{\rm core}$. This is due to the competition between thermal radiation from the cloud core gas and total angular momentum of the protoplanetary disk+protostar system.
(4) The value of $R_{\max}$ increases monotonically with the mass of the molecular cloud core $M_{\rm core}$. This is because when the disk region is extended to large radii, the increased mass $M_{\rm core}$ resupplies material in the extended disk region, which makes the material denser.
(5) We compare the calculated $R_{\max}$ with the semimajor axes of extrasolar planets, and find that $R_{\max}$ may provide an upper limit for the locations of the formation of giant planets which are formed by the core accretion model. In Figure 5, extrasolar planets above the $R_{\max}$ curve are indeed rare. This may provide some support for our model.

Acknowledgements This work was supported by the National Natural Science Foundation of China (Grant No. 11504150).

References

Bacmann, A., André, P., Puget, J.-L., et al. 2000, A&A, 361, 555
Balbus, S. A., & Hawley, J. F. 1991, ApJ, 376, 214
Batygin, K., Bodenheimer, P. H., & Laughlin, G. P. 2016, ApJ, 829, 114

Bell, K. R., Cassen, P. M., Klahr, H. H., & Henning, T. 1997, ApJ, 486, 372
Bell, K. R., & Lin, D. N. C. 1994, ApJ, 427, 987
Cassen, P., & Moosman, A. 1981, Icarus, 48, 353
Chambers, J. E. 2006, ApJ, 652, L133
Ciesla, F. J., & Cuzzi, J. N. 2006, Icarus, 181, 178
Cuzzi, J. N., & Zahnle, K. J. 2004, ApJ, 614, 490
Dubrulle, B. 1993, Icarus, 106, 59
Dubrulle, B., Marié, L., Normand, C., et al. 2005, A&A, 429, 1
Fleming, T., & Stone, J. M. 2003, ApJ, 585, 908
Fukue, J. 2013, Progress of Theoretical and Experimental Physics, 2013, 053E02
Gammie, C. F. 1996, ApJ, 457, 355
Gammie, C. F. 2001, ApJ, 553, 174
Goodman, A. A., Benson, P. J., Fuller, G. A., & Myers, P. C. 1993, ApJ, 406, 528
Haghighipour, N., & Boss, A. P. 2003, ApJ, 598, 1301
Haisch, Jr., K. E., Lada, E. A., & Lada, C. J. 2001, ApJ, 553, L153
Hayashi, C. 1981, Progress of Theoretical Physics Supplement, 70, 35
Hueso, R., & Guillot, T. 2005, A&A, 442, 703
Ida, S., & Lin, D. N. C. 2004, ApJ, 604, 388
Jijina, J., Myers, P. C., & Adams, F. C. 1999, ApJS, 125, 161
Jin, L., & Sui, N. 2010, ApJ, 710, 1179
Klahr, H. H., & Bodenheimer, P. 2003, ApJ, 582, 869
Kratter, K. M., Matzner, C. D., & Krumholz, M. R. 2008, ApJ, 681, 375
Kretke, K. A., & Lin, D. N. C. 2007, ApJ, 664, L55
Laughlin, G., & Bodenheimer, P. 1994, ApJ, 436, 335
Laughlin, G., & Rozyczka, M. 1996, ApJ, 456, 279
Lin, D. N. C., & Papaloizou, J. 1986, ApJ, 309, 846
Lissauer, J. J. 1993, ARA&A, 31, 129
McKee, C. F., & Ostriker, E. C. 2007, ARA&A, 45, 565
Motte, F., Andre, P., & Neri, R. 1998, A&A, 336, 150
Nakamoto, T., & Nakagawa, Y. 1994, ApJ, 421, 640
Pollack, J. B., Hubickyj, O., Bodenheimer, P., et al. 1996, Icarus, 124, 62
Podolak, M., & Mekler, Y. 1997, Planet. Space Sci., 45, 1401
Podolak, M., & Zucker, S. 2004, Meteoritics and Planetary Science, 39, 1859
Richard, D. 2003, A&A, 408, 409
Shakura, N. I., & Sunyaev, R. A. 1973, A&A, 24, 337
Shu, F. H. 1977, ApJ, 214, 488
Stepinski, T. F., & Valageas, P. 1997, A&A, 319, 1007
Stevenson, D. J., & Lunine, J. I. 1988, Icarus, 75, 146
Toomre, A. 1964, ApJ, 139, 1217
Umebayashi, T. 1983, Progress of Theoretical Physics, 69, 480
Zhang, K., Blake, G. A., & Bergin, E. A. 2015, ApJ, 806, L7
Zhang, Y., & Jin, L. 2015, ApJ, 802, 58
Zhu, Z., Hartmann, L., Nelson, R. P., & Gammie, C. F. 2012, ApJ, 746, 110